

# DESIGN AND OPERATION OF 1<sup>st</sup> AND 2<sup>nd</sup> HARMONIC COAXIAL GYROKLYSTRONS FOR ADVANCED ACCELERATOR APPLICATIONS

W. Lawson, M. Castle, J. Cheng, V. L. Granatstein, B. Hogan, M. Reiser, and X. Xu,  
University of Maryland, College Park, MD 20742 USA

## Abstract

We are currently conducting a series of experiments on coaxial gyroklystron tubes that are designed to produce peak powers in excess of 100 MW in X- and Ku-Band. Calibrated measurements have indicated peak powers in excess of 75 MW at 8.6 GHz in a three-cavity first harmonic tube with a gain near 30 dB and efficiency near 32%. In this paper we detail the results of this tube. We also discuss designs and cold test results of a three-cavity second harmonic device, which is predicted to give comparable results at 17.14 GHz.

## 1 INTRODUCTION

At the University of Maryland, we have been investigating the suitability of high power gyro-amplifiers as drivers for linear colliders for over a decade. [1] To this end, we have designed, constructed, and tested a variety of gyroklystron and gyrotwystron tubes operating from X-Band to Ka-Band. With a 440 kV, 160-260 A beam, we were able to produce about 30 MW of peak power in 1  $\mu$ s pulses near 9.87 and 19.7 GHz with first and second harmonic gyroklystron tubes, respectively. The peak efficiencies were near 30% and the large-signal gains were 25-35 dB. Circular electric modes were used in all cavities and the average beam velocity ratio was always near one. Efficiency was limited by instabilities in the beam tunnel preceding the input cavity and beam power was limited by the electron gun.

The focus in the past few years has been to upgrade the system to achieve peak powers approaching 100 MW in X- and Ku-Band. The increase in power results from a larger beam current, which is achieved by maintaining the same current density, but enlarging the average beam radius. Subsequently, the tube cross-sectional dimensions are increased and an inner conductor is required to maintain cutoff to the operating mode in the drift regions. We have currently tested both a 2-cavity and a 3-cavity first harmonic tube. However, the 2-cavity system was gain-limited to a power below 1 MW. Therefore we describe here only the 3-cavity results.

In this paper we first discuss the experimental test facility. Then we discuss the computer simulations before

describing the experimental results from our X-Band tube. Finally, we mention our Ku-Band progress before closing with our near and long term goals.

## 2 EXPERIMENTAL TEST FACILITY

The voltage pulse is generated with a line-type modulator which is capable of producing 2  $\mu$ s flat-top pulses at up to 2 Hz with voltages and currents up to 500 kV and 800 A, respectively. A capacitive voltage divider and a current transformer are used to measure the time evolution of the voltage and current. Our single-anode

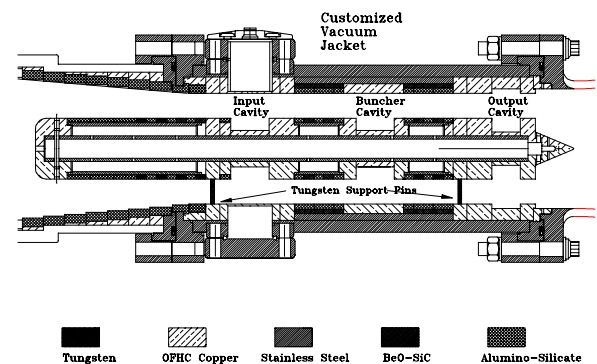


Figure 1. The three-cavity microwave circuit.

MIG is capable of producing a 500 kV, 720 A beam with an average orbital-to-axial velocity ratio of  $\alpha = 1.5$  and an axial velocity spread of less than 10%. The beam parameters are given in Table I for the operating point where maximum amplification occurs. The voltage and current are measured quantities; all other values come from the EGUN simulations and are based on the MIG geometry and the magnetic field profile. The actual theoretical fields at the centers of the three cavities are given in Table I. The axial field is detuned by about -3.5% in the input cavity, -8.8% in the buncher cavity and -15.4% in the output cavity.

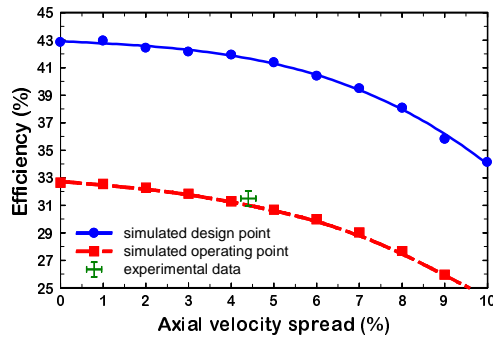


Figure 2. Efficiency versus velocity spread.

Table I. The system parameters.

Beam parameters	
Beam Voltage (kV)	470
Beam Current (A)	505
Average Velocity Ratio	1.05
Axial velocity spread (%)	4.4
Average beam radius (cm)	2.38
Magnetic field parameters	
Input cavity field (kG)	5.69
Buncher cavity field (kG)	5.38
Output cavity field (kG)	4.99
Input cavity parameters	
Inner radius (cm)	1.10
Outer radius (cm)	3.33
Length (cm)	2.29
Quality factor	65 ± 10
Buncher cavity parameters	
Inner radius (cm)	1.10
Outer radius (cm)	3.33
Length (cm)	2.29
Quality factor	75 ± 10
Output cavity parameters	
Inner radius (cm)	1.01
Outer radius (cm)	3.59
Length (cm)	1.70
Quality factor	135 ± 10
Drift tube parameters	
Inner radius (cm)	1.83
Outer radius (cm)	3.33
Length (between I-B) (cm)	5.18
Length (between B-O) (cm)	5.82
Amplifier Results	
Drive Frequency (GHz)	8.60
Output power (MW)	75
Pulse length (μs)	1.7
Gain (dB)	29.7
Efficiency (%)	31.5

The microwave circuit is shown in Fig. 1. The key dimensions are given in Table I. The inner conductor is supported by two 2 mm diameter tungsten pins, which

intercept approximately 3% of the beam. The primary function of the inner conductor is to force the drift tubes to be cutoff to the operating mode. The inner conductor only extends a few centimeters into the downtaper and is rapidly terminated after the output cavity. Lossy ceramics are placed in the drift regions to help suppress spurious modes. The rings on the inner conductor generally alternate between carbon-impregnated alumino-silicate (CIAS) and 80% BeO-20% SiC. Two layers of lossy ceramics are placed along the outer conductor in the drift regions. The outer layer is BeO-SiC and the inner layer is CIAS.

The input cavity is defined by a decrease in the inner conductor radius and has a length that matches the width of X-band waveguide. The cavity loss is roughly evenly divided between the diffractive loss of the coupling aperture and the ohmic loss of the cavity. The latter loss is provided by a CIAS ring on the inner conductor which is placed adjacent to the cavity and is separated by a thin copper section which is adjusted to produce the proper Q. The power to the input cavity is supplied by a 150 kW coaxial magnetron. The buncher cavity has identical dimensions for the metal components. However, the Q is determined entirely by the ohmic loss of the adjacent CIAS ceramics. The output cavity is defined by radial changes on both walls and the lip radii are equal to the drift tube radii. The quality factor is dominated by the diffractive Q, which is adjusted by changing the length of the coupling lip.

### 3 FIRST HARMONIC RESULTS

A partially self-consistent large-signal code is used to design the circuit and magnetic field configuration and to estimate the performance of the tube at the actual operating point. A small-signal start-oscillation code is used to determine the stability properties of the cavities and set limits on the cavity quality factors. The solid line in Fig. 2 shows the expected performance of the tube as a function of velocity spread for  $\alpha=1.5$ . The simulation predicts a zero-spread efficiency of 43%, and an efficiency of 34% for 10% spread. For the 6% spread predicted for a 500 A beam, the simulated interaction efficiency is about 40%. All microwave cavities are expected to be stable at the design operating point for the quality factors indicated in Table I.

The optimal parameters and experimental results have been listed in Table I. The values are all taken from anechoic chamber measurements. The time dependence of the beam voltage (dashed line), beam current (dot-dashed line), and the amplified signal (solid line) are shown in Fig. 3. There is a slight droop on the flat top due to a mismatch with the modulator impedance. The peak values indicated in Table I represent the average values of the signals in the flat top region. The peak power is about 75 MW, which represents an efficiency of nearly 32%. The corresponding gain is almost 30 dB and the pulse width is 1.7 μs (FWHM). Attempts to increase the peak power

further by raising the beam's velocity ratio result in a sharp cut in the output signal near the maximum value, which is usually indicative of instability (though none were detected by the microwave diagnostics).

An EGUN simulation using the parameters of the operating point indicates that the beam's velocity ratio at the entrance to the circuit is near one. There is a reasonably large uncertainty in this ratio due to the neglect of the self-axial magnetic field in EGUN and the uncertainty in the applied field at the cathode. In a previous experiment at the University of Maryland, for example, the measured average velocity ratio was consistently higher than the simulated ratio by about 15%. [2] Simulations of the amplifier performance at the operating point are given by the dashed line in Fig. 2. The simulated cathode magnetic field is adjusted slightly to produce the best match between the theoretical efficiency and the measured efficiency, which is indicated by the cross. The required field is about 20 G lower than the calculated ideal field and well within the uncertainties of the experimental data.

## 4 SECOND HARMONIC TUBE

The second harmonic tube is realized by keeping the first harmonic tube's input cavity essentially the same (the Q was lowered by 25%) but replacing the buncher and output cavities with ones that resonate at twice the drive frequency in the  $TE_{021}$  mode. Such cavities are normally difficult to realize, because the cavities end walls generate other radial modes due to the beam tunnel opening. For cavity isolation, the fields must not leak substantially into the drift regions, yet the operating frequency is well above the cutoff of the  $TE_{01}$  mode. In circular waveguide systems, the usual way to avoid this problem is to introduce smoothly varying wall radii, but the added length of these transitions is usually unacceptable. Fortunately, in coaxial tubes, making the radial wall transitions that define the  $TE_{021}$  cavity approximately equal on the inner and outer walls naturally leads to a mode with very little conversion to the  $TE_{01}$  modes and subsequent leakage fields.

The principal design parameters for our three cavity 2<sup>nd</sup> harmonic tube are given in Table II along with the simulated performance estimates. The drift region lengths are close to those of the first harmonic tube. The lengths of the buncher and output cavity are about 1.7 cm each. At this point, the tube has been entirely constructed, the cavities have been adjusted to achieve the required frequencies and quality factors, and we are currently installing the tube in our test facility. Hot testing should commence in the next few weeks.

## 5 SUMMARY

In summary, we have developed an X-band coaxial gyrokylystron, which has increased the state-of-the-art in peak power for gyrokylystrons by nearly a factor of 3. In the near future we will test our 2<sup>nd</sup> harmonic tube with the goal of obtaining about 100 MW of peak power at 17.136 GHz. We will investigate the limitations on velocity ratio in greater detail and attempt to increase the nominal velocity ratio to the original design value and increase the efficiency to 40%. In the long term we expect to build a high-gain, high repetition rate-capable gyrokylystron, and build and power a 17.136 GHz accelerator structure with an accelerating gradient near 200 MV/m.

## 6 ACKNOWLEDGEMENTS

This work was supported by the U. S. Department of Energy.

Table II. The 2<sup>nd</sup> harmonic design.

Beam voltage (kV)	500
Beam current (A)	770
Velocity ratio	1.51
Input cavity Q	50
Buncher cavity Q	389
Output cavity Q	320
Gain (dB)	49
Efficiency (%)	41
Output power (MW)	158

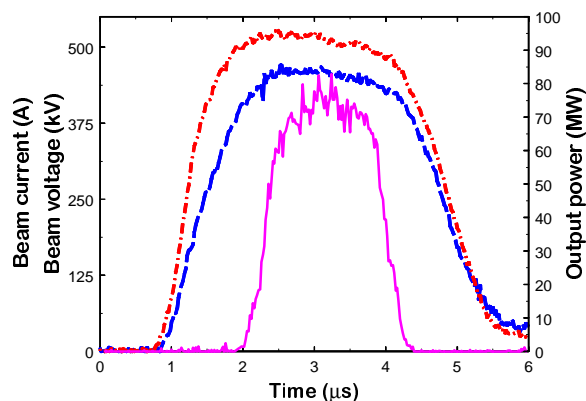


Figure 3. Time dependence of the output pulse.

## REFERENCES

- [1] V. L. Granatstein and W. Lawson, *IEEE Trans. on Plasma Science*, vol. 24, p. 648 (1996).
- [2] J. P. Calame and W. Lawson, *IEEE Trans. Electron Devices*, vol. 38, p. 1538 (1991).